Journal of Environmental Health Science and Engineering (2020) 18:1581–1593
https://doi.org/10.1007/s40201-020-00576-8

RESEARCH ARTICLE

Green synthesis of SnO_2-ZnO-eggshell nanocomposites and study of their application in removal of mercury (II) ions from aqueous solution

Marieh Honarmand[1] · Mohammad Mirzadeh[2] · Moones Honarmand[2]

Received: 24 March 2020 / Revised: 21 September 2020 / Accepted: 15 October 2020 / Published online: 25 October 2020

Abstract

Background Mercury (Hg) in dental amalgam is the world's hidden source of mercury contamination. The development of more eco-friendly and cost-effective adsorbents to reduce mercury pollutants in wastewater is highly desirable and is still a major challenge. In this study, a novel nanocomposite was synthesized and used as an efficient adsorbent for the removal of Hg(II) ions from aqueous solution.

Methods A green and cost-effective method was described to the synthesis of SnO_2-ZnO-eggshell nanocomposites using teucrium polium extract as a renewable reductant and mild stabilizer. The biosynthesized nanocomposites were characterized by various techniques. The novel SnO_2-ZnO-eggshell nanocomposites were used as an effective adsorbent in the removal of mercury (II) ions. To achieve the maximum absorption efficiency of Hg(II) ions, the effect of operating factors such as pH value, the dose of catalyst, the initial metal concentration of Hg(II) ions, and catalyst type were evaluated.

Results The removal percentage and adsorption capacity of Hg(II) were obtained 99.15% and 396.6 $mg.g^{-}1$, respectively, under optimal conditions after 5 minutes. The selectivity of SnO_2-ZnO-eggshell nanocomposites for the adsorption of metal ions was studied, and the highest selectivity was obtained for adsorption of Hg (II) ions. Furthermore, the SnO_2- ZnO-eggshell nanocomposites could be recovered and reused at least three times without considerable loss of their efficiency.

Conclusions The present approach has advantages such as rapidity, simplicity, selectivity, low cost and, most importantly, the use of nanocomposites containing a bio-waste material of eggshell for removal of Hg(II) ions from aqueous solution.

Keywords SnO_2-ZnO-eggshell nanocomposites · Teucrium polium · Mercury · Adsorbent · recyclable · Selectivity

Introduction

For over 170 years, mercury (Hg) has been utilized as a dental amalgam for teeth filling in dentistry. Based on the World Health Organization (WHO) report, the highest human exposure to mercury is from dental amalgams. Extensive use of mercury in dentistry has resulted in the release of hundreds of tons of mercury into discharge systems, which can generate ionic mercury. The most toxic form of mercury is in its ionic species which mercury ions react with the biomolecules of a living being body and form very stable toxic bio-compounds [1–4]. Given these worrying statistics, how Hg(II) ions are removed from wastewater is a significant concern worldwide. Nowadays, various technologies have been put forward to remove Hg(II) ions such as biological treatment, precipitation, chemical reduction, ion-exchange, extraction, electrolytic accumulation, filtration, membrane technique, and adsorption methods [5–8]. Among these methods, adsorption is more effective and practical than other techniques [9]. Therefore, the increasing use of adsorption techniques has necessitated the development of recyclable and cost-effective adsorbents for the better removal of Hg(II) ions from contaminated media.

In recent years, nanotechnology appears as a new innovative technology with excellent potential for wastewater treatment in the natural environment through more effective strategies than previously explored methods [10–13]. In this

✉ Moones Honarmand
honarmand@birjandut.ac.ir; honarmand.moones@yahoo.com

[1] Oral and Dental Disease Research Center, Department of Oral Medicine, School of Dentistry, Zahedan University of Medical Sciences, Zahedan, Iran

[2] Department of Chemical Engineering, Birjand University of Technology, Birjand, Iran

regard, nanoparticles have attracted researchers' attention due to their interesting properties such as large specific surface area, low cost, high stability and very small size. Among the various types of nanoparticles, metal oxide nanoparticles such as tin oxide (SnO_2) and zinc oxide (ZnO) nanoparticles exhibited good activity in wastewater treatment [14–16]. There are various physicochemical techniques for the fabrication of these nanoparticles including thermal reduction [17, 18], chemical vapor synthesis [19, 20], sol-gel [21, 22], radiation methods [23, 24], microemulsion techniques [25, 26], laser ablation [27, 28] and mechanical attrition [29, 30]. Most of these methods have shortcomings such as low purity, harsh reaction conditions, production of side products, and the use of complicated equipment, toxic solvents and hazardous chemicals. So, it is desirable to develop more cost-effective and environmental-friendly approaches for the synthesis of metal oxide nanoparticles under mild conditions. The green synthesis of nanoparticles using natural and renewable materials like plant extract has advantages such as milder and cleaner conditions, and avoidance of expensive organic solvents and hazardous reagents [16, 31, 32].

Teucrium polium belongs to the Lamiaceae family and their shrubs grow in North Africa, Asia and Europe. From a long time ago, Teucrium polium has been used to treat gastrointestinal diseases, inflammation, diabetes and rheumatism. The phytochemical studies have shown which the main constituent of this plant is flavonoids [33]. The presence of these compounds in Teucrium polium induces excellent reducing properties to it that makes Teucrium polium extract as an excellent reducing agent and green media for the synthesis of nanoparticles [34].

In both chemical and green synthesis of nanoparticles, the major problem is the agglomeration of nanoparticles because of their small size. One of the best methods to overcome this problem is use natural suitable supports for the deposition of metal oxide nanoparticles and formation of nanocomposites such as TiO_2/zeolite [35], SnO_2/bentonite [36], Fe_3O_4/starch [37], FeO/chitosan [38], ZnO/cellulose [39], ZnO/alginate [39], $MnFe_2O_4$/diatomite [40], gelatin/TiO_2[41] and graphene oxide/ZnO [42]. If the purpose of synthesizing a nanocomposite is to absorb pollutants, it would be valuable to use a support that has high adsorption property.

In recent years, researchers were used many agricultural and biological waste materials such as rice husk [43], eggshell [44], Moringa pods [45], bamboo leaf powder [46], cashew nut shells [47] and palm oil fruit shells [48] as low-cost adsorbents for the removal of heavy metals from aqueous medium. The eggshell could be a right choice as support because of its intrinsic porous structure. The eggshell is a cheap and readily available bio-waste. It is particularly attractive for the synthesis of nanocomposites due to the formation of strong metal-protein bonds between the eggshell and nanoparticles [49].

Since our goal in this study is the adsorption of Hg(II) ions using nanoparticles, and due to the excellent performance of SnO_2 and ZnO nanoparticles in the removal of contaminants from wastewater [14, 50], to benefit the fantastic properties of SnO_2 and ZnO nanoparticles, we decided to the synthesis of SnO_2-ZnO nanocomposites based on the principles of green chemistry. On the other, to prevent the agglomeration of nanoparticles, we selected eggshells as natural support for nanoparticles which itself acts as an efficient adsorbent. Therefore, we synthesized SnO_2-ZnO-eggshell nanocomposites *via* a facile and non-toxic method using Teucrium polium extract as a renewable reducing agent and efficient stabilizer. Then, the activity of the SnO_2-ZnO-eggshell nanocomposites was studied in the removal of Hg(II) ions from aqueous solution. The SnO_2-ZnO-eggshell nanocomposites exhibited highly excellent catalytic performance in the adsorption of Hg(II) ions at room temperature. Moreover, the SnO_2-ZnO-eggshell nanocomposites could be recovered three times without considerable loss of catalytic activity. To our knowledge, the green synthesis of SnO_2-ZnO-eggshell nanocomposites has not been reported in the literature.

Experimental

Materials

The tin (II) chloride dehydrate ($SnCl_2.2H_2O$), zinc nitrate hexahydrate [$Zn(NO_3)_2.6H_2O$] and mercury(II) chloride ($HgCl_2$) were purchased from Sigma-Aldrich and Fluka companies. Teucrium polium plant was collected from the deserts of South Khorasan in Iran. The eggs were purchased from the local supermarket.

Characterization techniques

The crystal structure and composition of SnO_2-ZnO-eggshell nanocomposites was studied by X-ray diffraction (XRD) on a Philips model PW 1800 X'pert diffractometer. The shape and particle size distribution of the SnO_2-ZnO-eggshell nanocomposites were specified by Transmission Electron Microscopy (TEM- ZEISS EM900). Energy dispersive X-ray spectroscopy (EDS-ZEISS, EVO18) and scanning electron microscopy (SEM-ZEISS, EVO18) analyses were carried out to study the elemental composition and morphology of SnO_2-ZnO-eggshell nanocomposites and other compounds. The concentration of Hg(II) in the solutions after adsorbent exposure was investigated by inductively coupled plasma-light emission spectroscopy (ICP-OES, ES-730).

Preparation of the Teucrium polium extract

The dried powder of Teucrium polium leaves (10 g) was refluxed using distilled water (100 mL) at 80 °C for 45 minutes. The Teucrium polium extract was filtered and used for the green synthesis of nanomaterials in the next steps.

Biosynthesis of SnO_2 nanoparticles

The extract of Teucrium polium (50 mL) was dropped into a well-mixed solution of tin (II) chloride dihydrate (25 mL, 0.05 M) with constant stirring at laboratory temperature for 30 minutes. The resulting mixture was magnetostirred for another 30 minutes at 70 °C. In the following, the reaction mixture was cooled and the synthesized precipitates were centrifuged at 10,000 rpm and rinsed three times with double distilled water and dried at laboratory temperature. The biosynthesized nanocomposites were powdered using a mortar and placed in an electric furnace at 550 °C for 2 h.

Biosynthesis of ZnO nanoparticles

The extract of Teucrium polium (180 mL) was dropped into a well-mixed solution of zinc nitrate hexahydrate (25 mL, 1 M) with constant stirring at laboratory temperature for 30 minutes. The resulting mixture was magnetostirred for another 8 h at 70 °C. The continuing the steps were quite similar to the one mentioned above.

Biosynthesis of SnO_2-ZnO-eggshell nanocomposites

The tin (II) chloride dihydrate solution (25 mL, 0.05 M), zinc nitrate hexahydrate (25 mL, 1 M), and crushed eggshell (1 g) was vigorously stirred for 30 minutes at laboratory temperature. The extract of the Teucrium polium (180 mL) was added drop-wise to the above well-mixed mixture for 30 minutes. The resulting mixture was magnetostirred for another 8 h at 70 °C. In the following, the reaction mixture was cooled and the synthesized precipitates were centrifuged at 10,000 rpm and rinsed three times with double distilled water and dried at laboratory temperature. The biosynthesized nanocomposites were powdered using a mortar and placed in an electric furnace at 550 °C for 2 h. The ZnO and SnO_2 loading in SnO_2-ZnO-eggshell nanocomposites was 1:0.05 (molar ratio ZnO:SnO_2).

Adsorption experiments

All adsorption tests were carried out with three replicates to examine the adsorption properties of SnO_2-ZnO-eggshell nanocomposites in the removal of Hg(II) from aqueous solutions. The experiments were done under different conditions such as pH values (2–7), initial metal concentration of Hg(II) ions (10-5000 $mg.L^{-1}$) and adsorbent amounts (0.001–0.05 g L^{-1}). The pH of solutions was adjusted using hydrochloric acid (HCl), sodium hydroxide (NaOH) solutions (0.1 M) and a pH-meter instrument (Metrohm, Switzerland). After the adsorption process, the SnO_2-ZnO-eggshell nanocomposites were separated by centrifugation and the concentration of Hg(II) ions in the solution phase was analyzed using ICP-OES. The following equations were used to evaluate the adsorptive capacity (Qe, $mg.g^{-1}$) and the removal percentage (E, %) of mercury (II), respectively:

$$Q_e = \frac{(C_0 - C_e)V}{m}$$

$$E = \frac{C_0 - C_e}{C_0} \times 100$$

In the above equations, C_0 and Ce are the initial and equilibrium concentration concentrations of mercury (II) ($mg.L^{-1}$) in solution, respectively. V (L) is the solution volume, and m (g) is the SnO_2-ZnO-eggshell nanocomposites dosage.

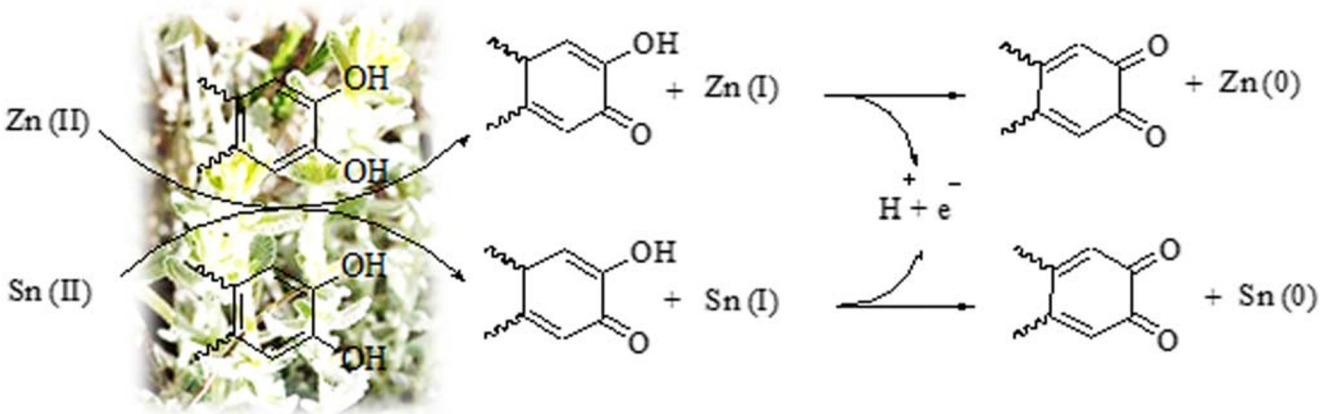

Scheme 1 The proposed mechanism for the green synthesis of Sn and Zn nanoparticles

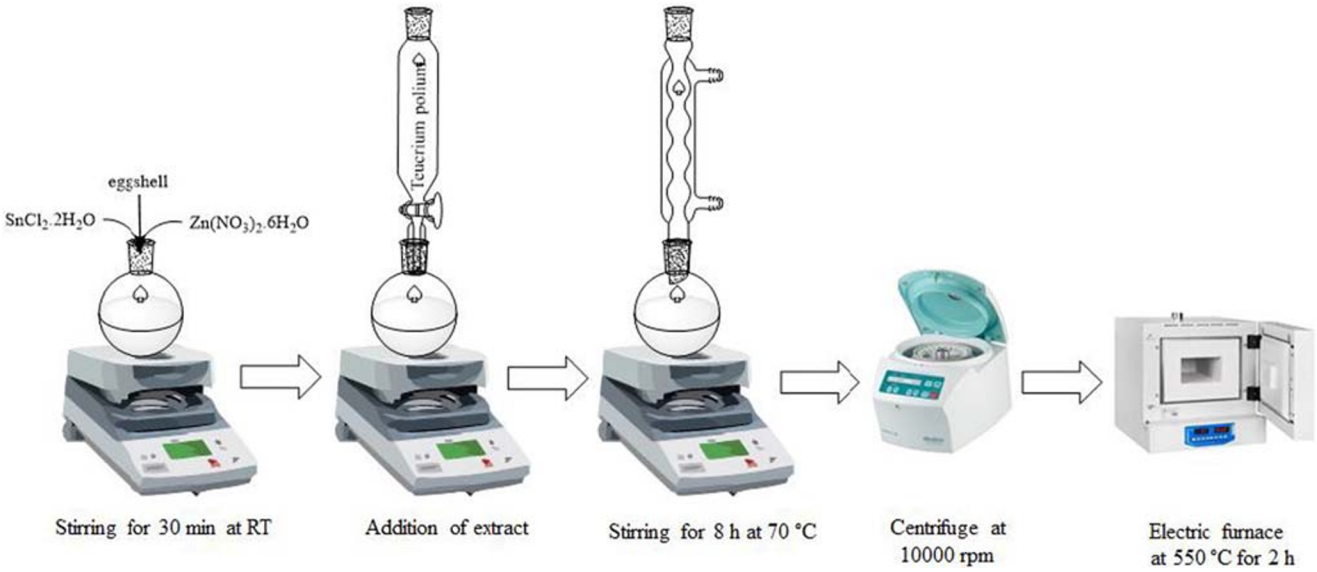

Fig. 1 Schematics of the green synthesis procedure of SnO_2-ZnO-eggshell nanocomposites using Teucrium polium

Desorption and regeneration studies

The desorption of Hg(II) was done using aqueous solutions of EDTA (0.05 M) as a suitable desorbing agent. After the adsorption process, the Hg(II) loaded nanocomposites were collected and agitated with the above desorbing agent (10 mL) for 5 h. Then the SnO_2-ZnO-eggshell nanocomposites were separated from the solution, washed three times with deionized water, dried at laboratory temperature and used again in the adsorption-desorption process the next three cycles.

Results and discussions

The aqueous extract of Teucrium polium leaves was used as an eco-friendly medium to the synthesis of SnO_2-ZnO-eggshell nanocomposites. The flavonoids in the extract of Teucrium polium leaves act as a green reducing agent and effectively reduced the Zn^{2+} and Sn^{2+} salt ions to Zn and Sn nanoparticles (Scheme 1). Also, the extract of Teucrium polium act as an efficient stabilizer and through the green reduction of Sn(II) and Zn(II) ions, were remarkably dispersed the formed nanoparticles in situ on the eggshell, and limited their agglomeration. The biosynthesized nanocomposites were finally obtained after calcination in an electric furnace at 550 °C for 2 h (Fig. 1). After the successful synthesis of SnO_2-ZnO-eggshell nanocomposites, the biosynthesized nanocomposites were employed as a green adsorbent to removal Hg(II) ions (Fig. 2).

The characterization of SnO_2-ZnO-eggshell nanocomposites

At first, to obtain information about the elemental composition of eggshell, SnO_2 nanoparticles, ZnO nanoparticles, and SnO_2-

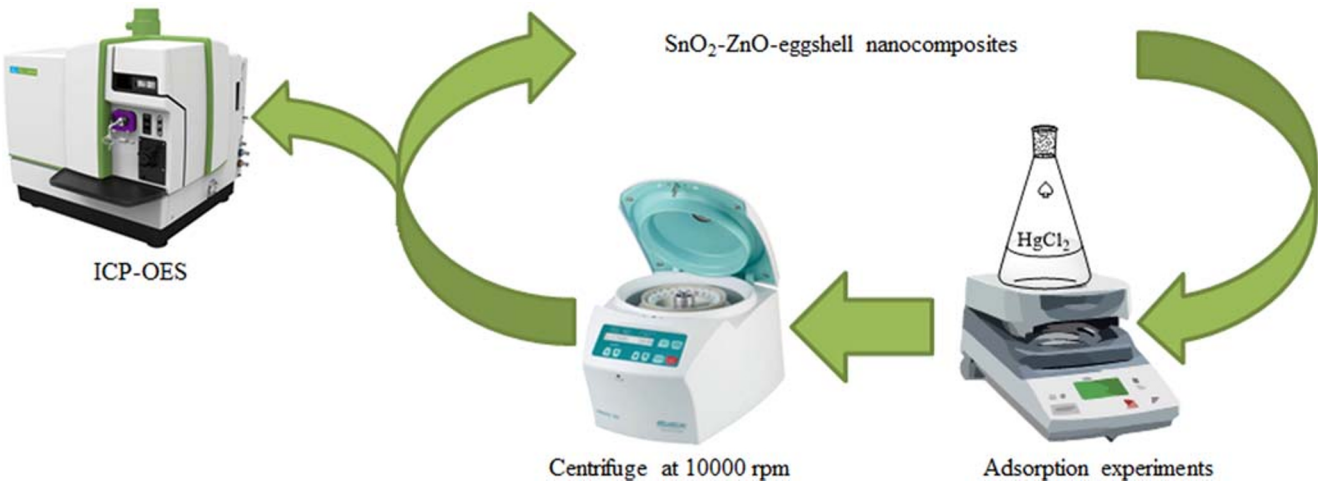

Fig. 2 Schematics of adsorption experiment of Hg ions using SnO_2-ZnO-eggshell nanocomposites

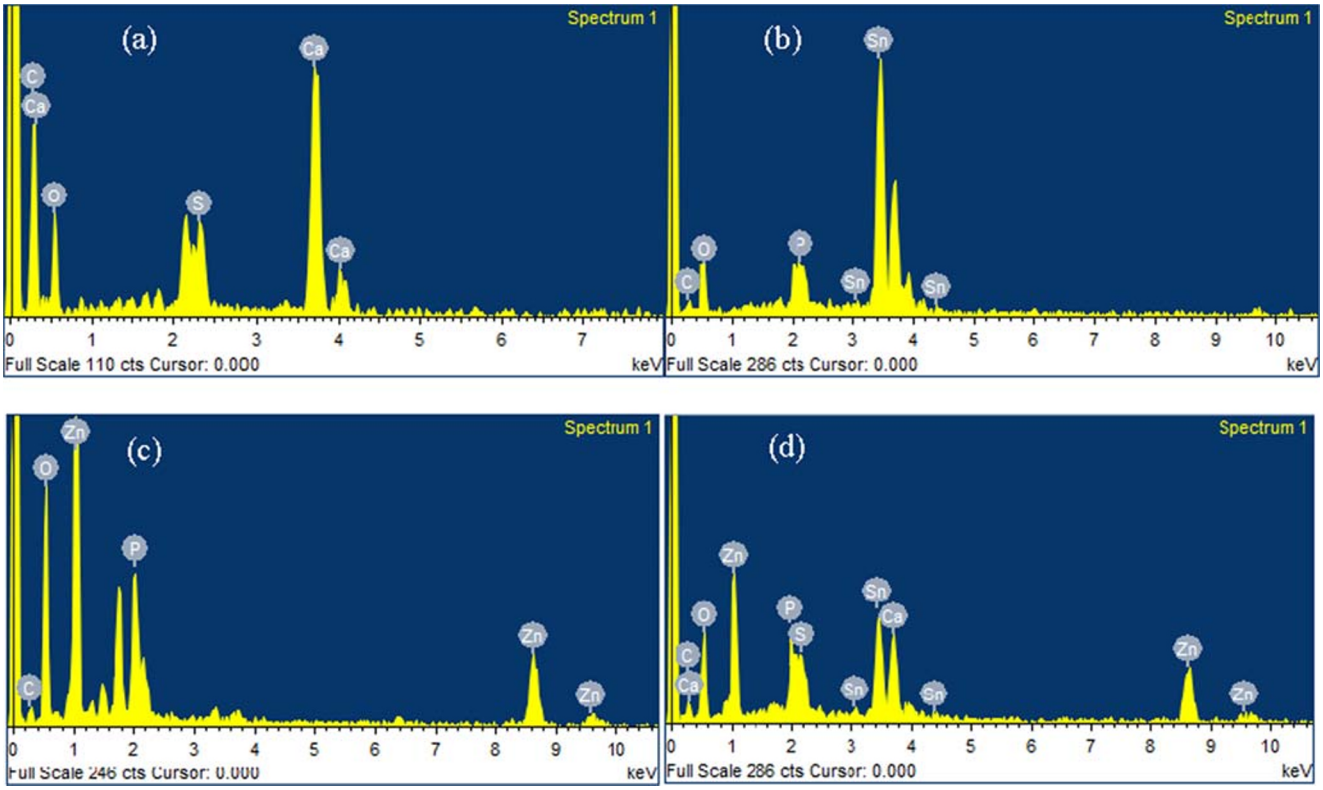

Fig. 3 EDX spectra of (**a**) eggshell, (**b**) SnO_2 nanoparticles, (**c**) ZnO nanoparticles and (**d**) SnO_2-ZnO-eggshell nanocomposites

ZnO-eggshell nanocomposites was done energy-dispersive X-ray spectroscopy (EDX) analysis (Fig. 3). The presence of carbon, oxygen, calcium and sulfur elements was determined in the EDX spectrum of the eggshell (Fig. 3a). The EDX spectra of the SnO_2 and ZnO nanoparticles were well indicated in the presence of tin, zinc and oxygen elements (Fig. 3b and c). The elements such as carbon and phosphorus with a low weight percentage in EDX spectra of the biosynthesized SnO_2 and ZnO nanoparticles were detected that were related to the used Teucrium polium extract in the synthesis process of nanoparticles. The presence of all the above elements in the EDX spectrum of SnO_2-ZnO eggshell nanocomposites indicated the successful synthesis of biosynthetic nanocomposites (Fig. 3d).

To understand the occurred morphological changes in the surface of the eggshell, SEM images of eggshell and SnO_2-ZnO-eggshell nanocomposites were recorded. As shown in Fig. 4a, eggshell is a macroporous network with interwoven fibers. Figure 4b shows the three-dimension structure of SnO_2-ZnO-eggshell nanocomposites in which eggshell was wholly coated with SnO_2 and ZnO nanoparticles.

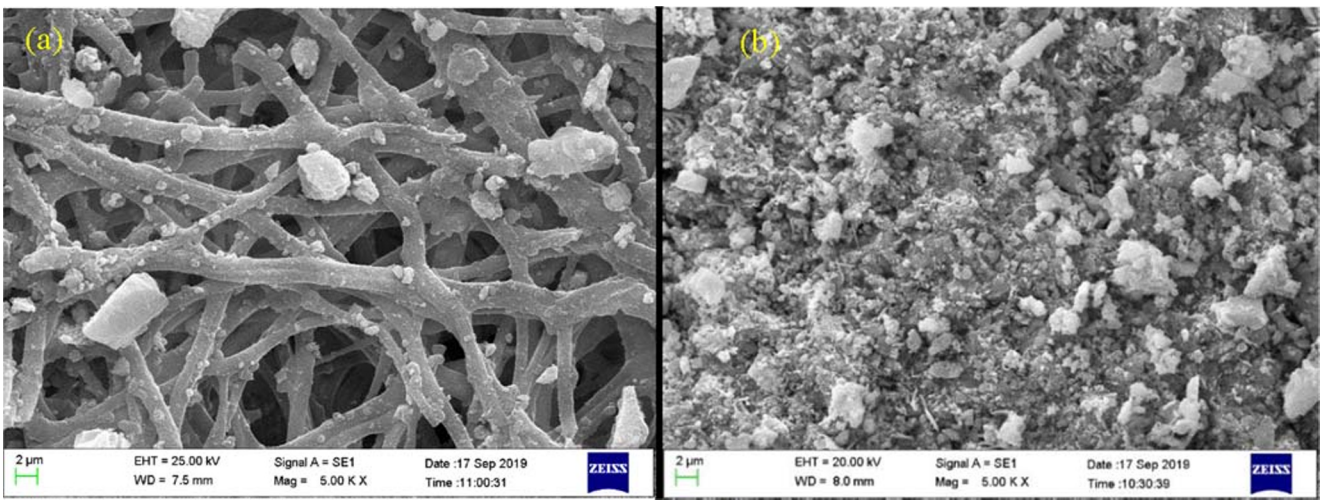

Fig. 4 SEM images of (**a**) eggshell and (**b**) SnO_2-ZnO-eggshell nanocomposites

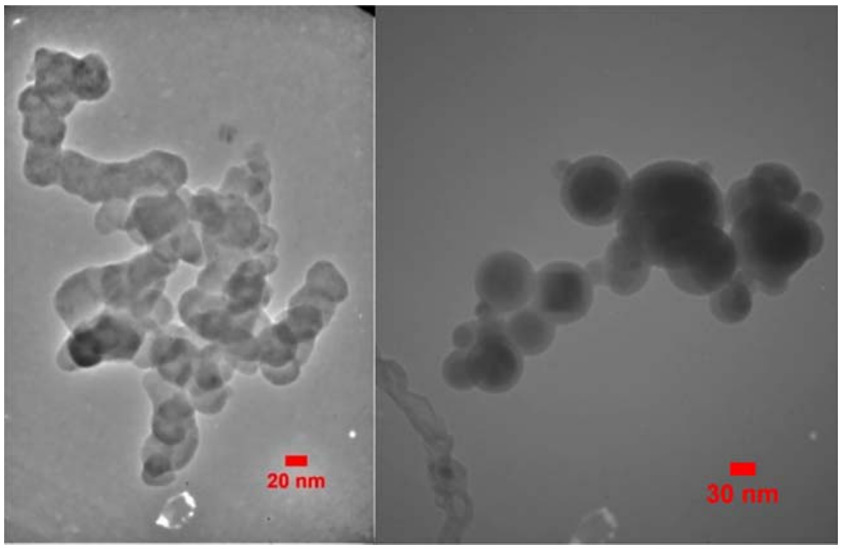

Fig. 5 TEM image of SnO_2-ZnO-eggshell nanocomposites

The TEM image of SnO_2-ZnO-eggshell nanocomposites demonstrated that biosynthesized nanocomposites have almost spherical morphology with homogeneous particle sizes in the range of 20–25 nanometer (Fig. 5).

The XRD patterns of the synthesized SnO_2-ZnO-eggshell nanocomposites were shown in Fig. 6. In the XRD pattern of eggshell, the strong and sharp peaks at $2\theta = 29.45°$, 36.04°, 39.49°, 43.03°, 47.76°, 48.65°, 57.55°, 60.89°, 64.67° and 68.99° could be indexed to (104), (110), (113), (202), (024), (116), (122), (214), (300) and (217) Bragg's reflections of rhombohedral $CaCO_3$ (JCPDS No. 00-002-0623) [51, 52]. To confirm the presence of SnO_2 nanoparticles in the biosynthesized nanocomposite, the typical XRD pattern showed diffraction peaks at 26.59°, 33.88°, 37.95°, 51.78°, 54.76°, 61.89°, 64.76° and 65.98° corresponding to (110), (101), (200), (211), (220), (310), (112) and (301) respectively (JCPDS No. 01-072-1147) [53]. The diffraction peaks at 31.69°, 34.33°, 36.10°, 47.36°, 56.31°, 62.64°, 67.64° and 68.73° were consistent with (100), (002), (101), (102), (110), (103), (112) and (201) reflections of the hexagonal phase of ZnO nanoparticles (JCPDS No. 01-079-0208) [54]. All of these peaks showed that SnO_2-ZnO-eggshell nanocomposites had been successfully prepared.

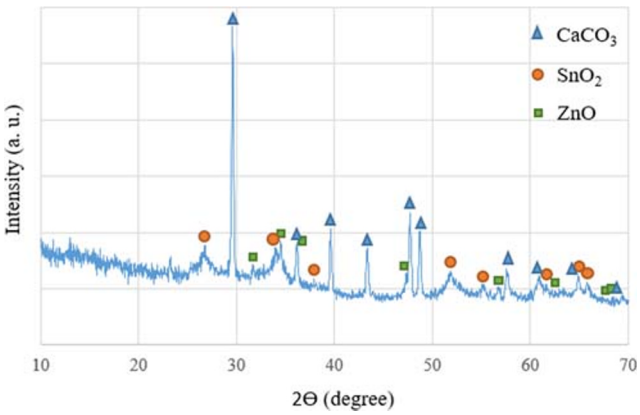

Fig. 6 XRD pattern of SnO_2-ZnO-eggshell nanocomposites

Based on the obtained results from TEM and XRD analysis and the definition of nanocomposite (nanocomposite is a multiphase solid material where one of the phases has one, two or three dimensions of less than 100 nanometers [55]), the naming of the nanocomposite for the biosynthesized compound was correct.

The adsorption of Hg(II) ions using biosynthesized SnO_2-ZnO-eggshell nanocomposites

Due to the undeniable toxicity of Hg(II) ions, in this work, the SnO_2-ZnO-eggshell nanocomposites were employed as a green adsorbent for removal of Hg(II) ions. The influence of several operating parameters such as pH values, the dose of catalyst, initial metal concentration of Hg(II) ions, catalyst type, existing other ions on adsorption capacity of Hg(II) using SnO_2-ZnO-eggshell nanocomposites was investigated.

Effect of pH

The pH value of solutions, in the adsorption process of pollutants, is one of the most significant parameters on adsorption capacity [12, 56]. Therefore, Hg(II) ions solution were prepared with different pH values (2, 3, 4, 5, 6 and 7) and their adsorption capacity was studied while other factors such as volume and concentration of the aqueous solution of $HgCl_2$ (100 mL, 20 $mg.L^{-1}$), the dose of catalyst (0.05 g) and temperature (laboratory temperature) were constant. The adsorption capacities of Hg(II) ions in different pH values were found to be around 361.2-396.6 $mg.g^{-1}$ with the standard deviation of 11.6 $mg.g^{-1}$. As shown in Fig. 7a, the adsorption capacity of Hg(II) ions onto SnO_2-ZnO-eggshell

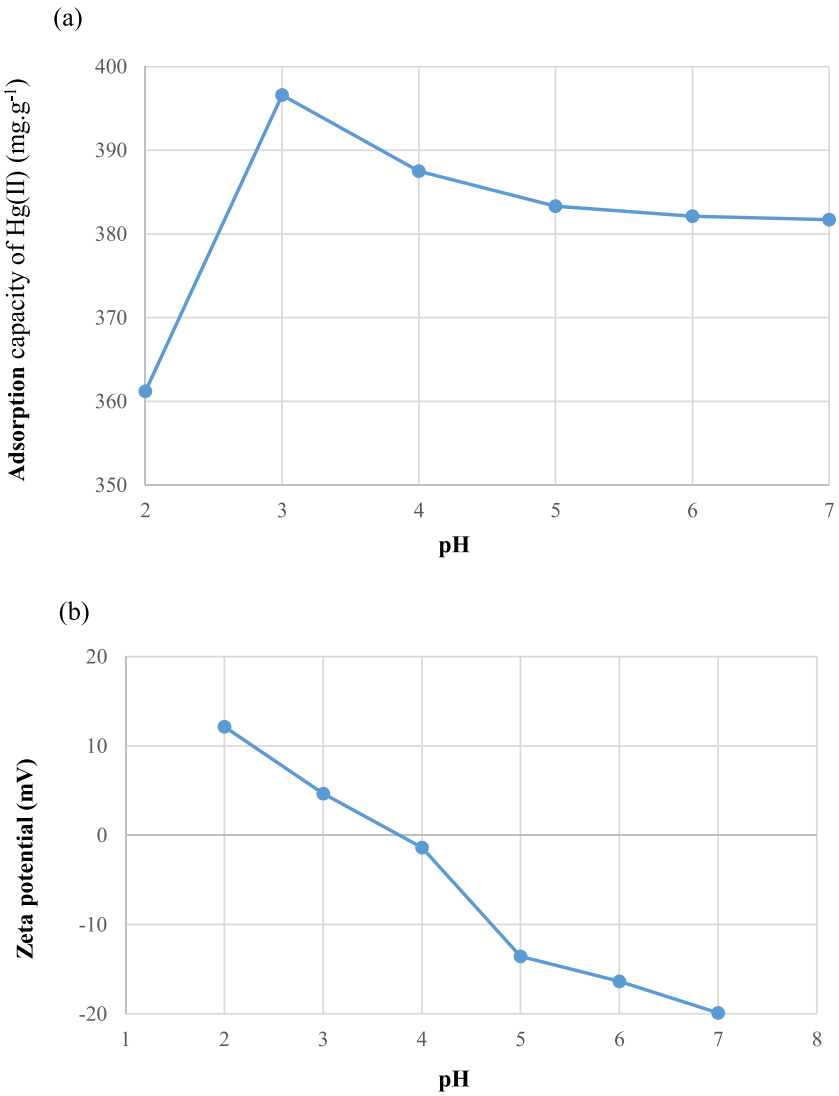

Fig. 7 Effect of pH on (**a**) adsorption capacity of Hg(II) using SnO_2-ZnO-eggshell nanocomposites ($C_0 = 200$ mg.L^{-1}, dosage of catalyst = 0.05 g, t = 5 min, and T = 298 K) and (**b**) Zeta potential of SnO_2-ZnO-eggshell nanocomposites

nanocomposites increased with increasing pH values first and then decreased slightly. At lower pH values, there are a large amount of H^+ ions in the solution, and they can compete with Hg(II) ions for the active sites on the surface of SnO_2-ZnO-eggshell nanocomposites and interfere in the adsorption process [57, 58]. When the pH values were more than 3, adsorption capacity was decreased because of the production of metal hydroxide of $Hg(OH)_2$ or $Hg(OH)^+$ [59]. Therefore, the maximum adsorption capacity of Hg(II) ions was obtained at pH value of 3 and after that, all of the experiments was carried out at pH = 3. At pH values greater than 8, metal hydroxides start to precipitate and the adsorption studies are practically impossible. Also, the zeta potential was applied to investigate the charge type on the surface of SnO_2-ZnO-eggshell nanocomposites in solutions with different pH values. The zeta potential values of SnO_2-ZnO-eggshell nanocomposites were shown in Fig. 7b. The isoelectric point was obtained when the pH value was 3.76. SnO_2-ZnO-eggshell nanocomposites have a positive charge when the pH value was less than 3.76 and have a negative charge when the pH value was higher than 3.76. The changes in the zeta potential of SnO_2-ZnO-eggshell nanocomposites showed which the electrostatic adsorption was not the main adsorption mechanism of Hg(II) ions by the biosynthesized nanocomposites [60].

Effect of dosage

The effect of dosage using newly SnO_2-ZnO-eggshell nanocomposites on the removal percentage and the adsorption capacity of Hg(II) ions was studied under the optimum conditions ($C_0 = 200$ mg.L^{-1}, pH = 3, t = 5 min, and T = 298 K) and the results were presented in Fig. 8. The selected dosages were 0.001, 0.005, 0.01, 0.025 and 0.05 g. The removal percentage of Hg(II) ions in different dosages was found to be around 84.91–99.15 mg.g^{-1} with the standard deviation of 5.78 mg.g^{-1}. The obtained results showed that the removal

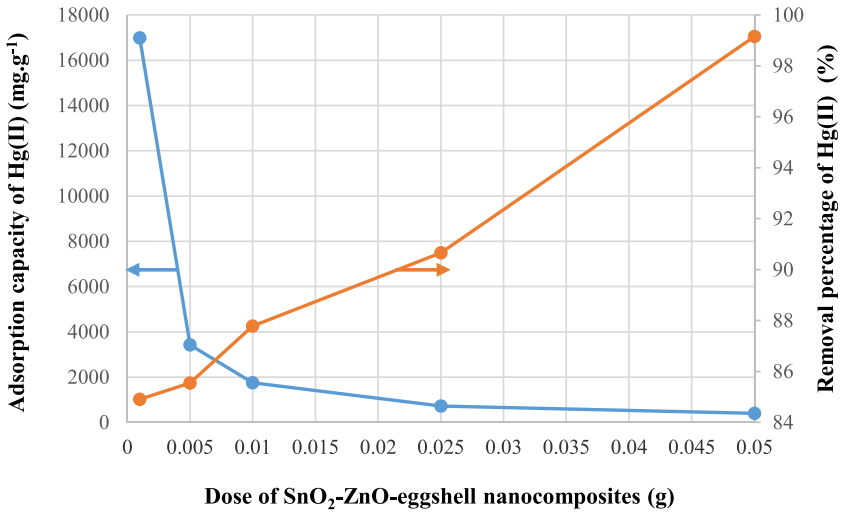

Fig. 8 Effects of dose of SnO_2-ZnO-eggshell nanocomposites ($C_0 = 200$ mg.L^{-1}, pH = 3, t = 5 min, and T = 298 K)

percentage of Hg(II) ions increased with an increasing dose of SnO_2-ZnO-eggshell nanocomposites, while adsorption capacity decreased. The increase in the adsorption percentage could be due to an increase in the number of available sites for adsorption of Hg(II) ions. However, in the case of a decrease in absorption capacity, it could be said with an increasing dose of SnO_2-ZnO-eggshell nanocomposites, active sites of adsorbent increase but the content of Hg(II) ions and the solution volume remain constant. The obtained results in this field were consistent with those reported in previous papers [61].

Effect of initial concentration

To study the effect of Hg(II) ions concentration on adsorption capacity, SnO_2-ZnO-eggshell nanocomposites (0.05 g) were immersed in solution (100 mL) at pH = 3 with initial Hg(II) ions concentrations of 100, 200, 500, 1000 and 5000 mg.L^{-1}, respectively. Then the solutions were stirred for 5 minutes. The adsorption capacities of Hg(II) ions in Hg(II) ions concentrations are found to be around 197.3-2229.7 mg.g^{-1} with a standard deviation of 1110.6 mg.g^{-1}. The obtained results are exhibited in Fig. 9. It could be found when the initial Hg(II) ions concentration increased from 100 to 5000 mg.L^{-1}, the adsorption capacity of Hg(II) increased. The increase of the adsorption capacity was because of the increase in the driving force of the concentration gradient [62].

Effect of catalyst type

To study the exact role of SnO_2-ZnO-eggshell nanocomposites on the adsorption capacity of Hg(II), the adsorption of Hg(II) ions were performed in the presence of SnO_2 nanoparticles, ZnO nanoparticles, eggshell and SnO_2-ZnO-eggshell nanocomposites. The adsorption capacity of Hg(II) using SnO_2 nanoparticles, ZnO nanoparticles, eggshell, and SnO_2-ZnO-eggshell

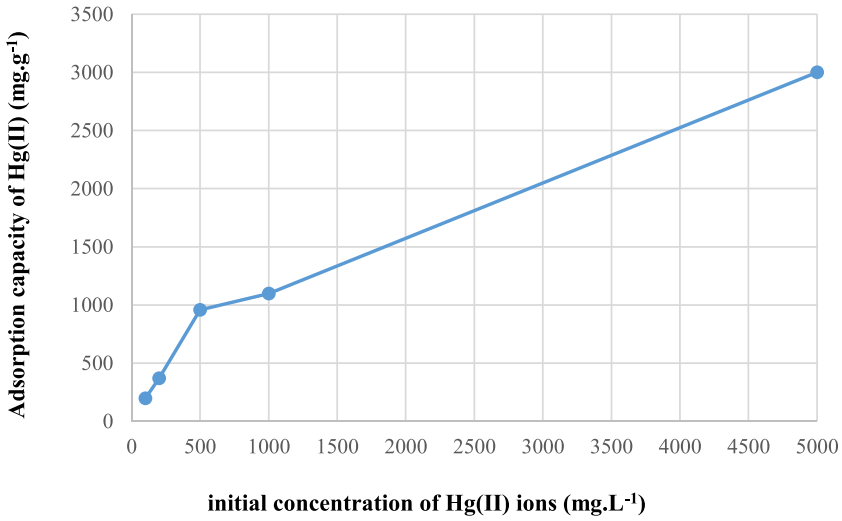

Fig. 9 Effects of initial concentration of Hg(II) ions (dose of catalyst = 0.05 g, pH = 3, t = 5 min, and T = 298 K)

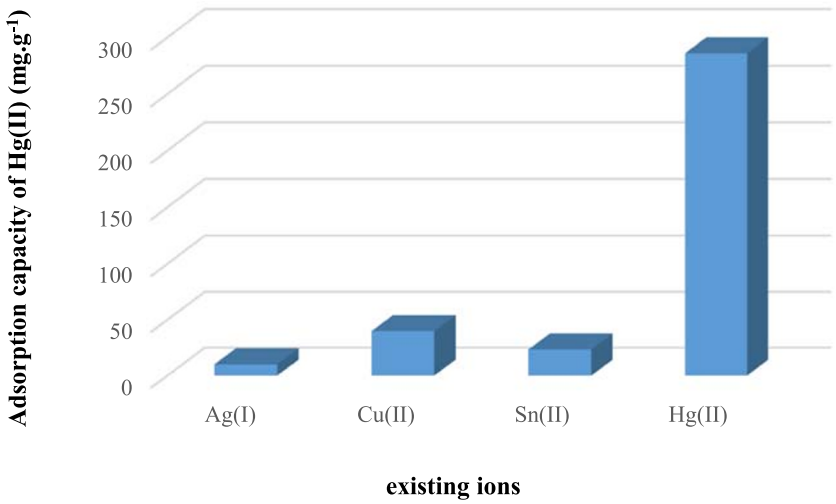

Fig. 10 Effects of existing ions (C_0 = 200 mg.L^{-1}, dose of catalyst = 0.05 g, t = 5 min, and T = 298 K)

nanocomposites were obtained 372.44, 366.82, 345.98 and 396.6 mg.g^{-1}, respectively, after 5 minutes. Surprisingly, all the components of the SnO_2-ZnO-eggshell nanocomposites were efficiently involved in the uptake of Hg(II) ions.

Effect of existing ions

The selectivity of SnO_2-ZnO-eggshell nanocomposites for adsorption of Hg(II) ions was carried out using the mixed metal ion solutions containing Ag, Cu, Sn and Hg chloride salts. These metal ions were chosen because they were components of dental amalgam. The concentration of each ion, dose of catalyst and pH were set at 200 ppm, 0.05 g and 3. The adsorption capacities of the mixed metal ions solution were shown in Fig. 10. The adsorption capacities for Ag(I), Cu(II), Sn(II) and Hg(II) ions were 10.15, 39.78, 23.43 and 285.96 mg.g^{-1}, respectively, with the standard deviation of 131.3 mg.g^{-1}. The obtained results clearly showed that the SnO_2-ZnO-eggshell nanocomposites have a higher selectivity for adsorption of Hg(II) ions than the other metal ions.

Comparison of the adsorption capacity with other adsorbents

To show the advantages of the SnO_2-ZnO-eggshell nanocomposites in the present work, a comparative study was performed between the SnO_2-ZnO-eggshell nanocomposites and other previously reported composites for the removal Hg(II). As shown in Table 1, among the reported composites, the highest adsorption capacity and shortest time in the removal of Hg(II) were obtained using SnO_2-ZnO-eggshell nanocomposites. Furthermore, the present study showed that the SnO_2-ZnO-eggshell nanocomposites were biosynthesized using the plant extract as a green reducing agent and safe stabilizing.

Table 1 Comparison of adsorption capacities of various composites for Hg(II)

Adsorbent	Adsorption capacity (mg.g^{-1})	Time (min)	Reference
MnO_2/CNT nanocomposites	58.8	80	[62]
Graphene oxide-Fe_3O_4 nanocomposite	16.6	120	[63]
Reduced graphene oxide-Ag	9	120	[64]
Fe_3O_4/poly ($C_3N_3S_3$) nanocomposite	344.8	60	[65]
Phytic acid doped polyaniline/cellulose acetate composite	280.11	600	[66]
Amino functionalized magnetic graphenes composite	23.03	200	[67]
2-Mercaptobenzamide modified itaconic acid-grafted-magnetite nanocellulose composite	240	60	[68]
Geopolymers modified with chitosan	156.01	60	[69]
Polyethylenimine modified-activated carbon	16.39	60	[70]
SnO_2-ZnO-eggshell nanocomposites	396.6	5	This study

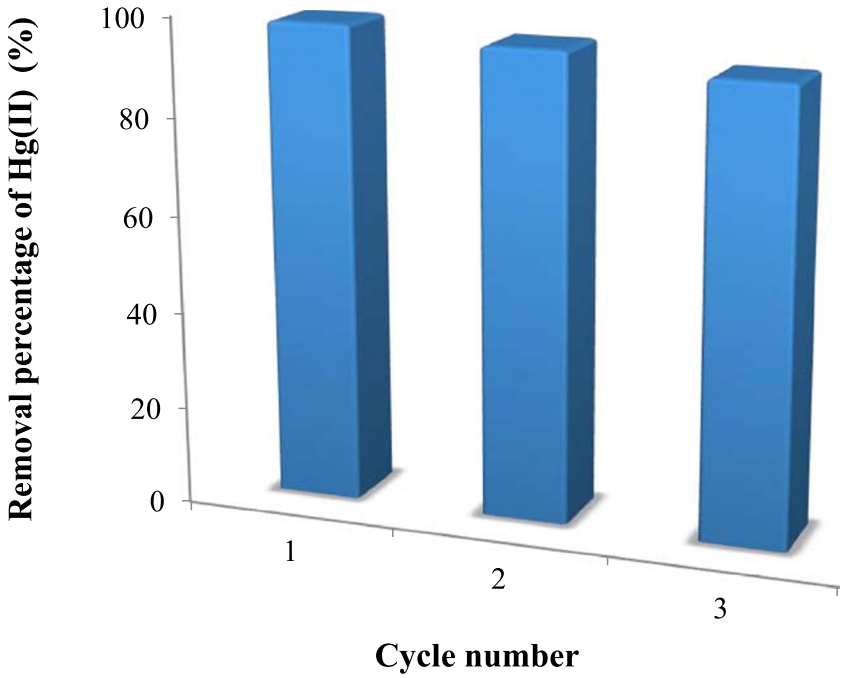

Fig. 11 Hg(II) adsorption efficiency using SnO_2-ZnO-eggshell nanocomposites in three consecutive cycles (C_0 = 200 mg.L^{-1}, dose of catalyst = 0.05 g, t = 5 min, and T = 298 K)

Reusability and stability of SnO_2-ZnO-eggshell nanocomposites

To have a cost-effective adsorbent, it must be reused several times in the adsorption-desorption cycles. For the desorption process and removing adsorbed Hg(II) ions from the adsorbent, firstly, used SnO_2-ZnO-eggshell nanocomposites were agitated with aqueous solutions of EDTA as a suitable desorbing agent. Then, SnO_2-ZnO-eggshell nanocomposites were separated from the reaction mixture, washed three times with water, dried and reused at least three times without any significant loss in their adsorption performance (Fig. 11). Furthermore, the stability of reused SnO_2-ZnO-eggshell nanocomposites was confirmed by TEM image (Fig. 12).

Conclusion

In this work, a simple procedure was described for the green synthesis of SnO_2-ZnO-eggshell nanocomposites using teucrium polium extract as a naturally-sourced reducing agent and efficient stabilizer. The SnO_2-ZnO-eggshell nanocomposites were characterized by EDX, SEM, TEM and XRD to study the chemical elemental composition, morphology and crystalline size of the biosynthesized nanocomposites. The SnO_2-ZnO-eggshell nanocomposites were employed as an efficient adsorbent for the removal of Hg(II) ions. The influence of several parameters, including pH value, the dose of catalyst, initial metal concentration of Hg(II) ions, catalyst type, existing other ions on adsorption capacity of Hg(II) using SnO_2-ZnO-eggshell nanocomposites were investigated. The obtained results confirmed the high ability of SnO_2-ZnO-eggshell nanocomposites in the removal of Hg(II) from aqueous solution, so that after only 5 minutes, the removal percentage and adsorption capacity approached to 100% and 400 mg.g^{-1}, respectively. The use of eggshell as a bio-waste and natural

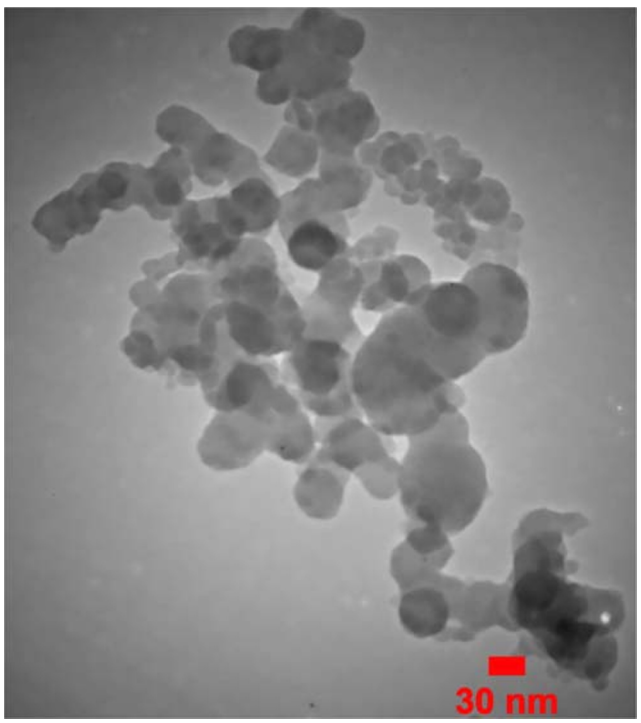

Fig. 12 TEM image of reused SnO_2-ZnO-eggshell nanocomposites after three times

support not only prevented the aggregation of SnO_2 and ZnO nanoparticles but also improved the adsorption activity of nanocomposite for efficient removal of Hg(II) ions. Furthermore, the SnO_2-ZnO-eggshell nanocomposites showed higher selectivity for adsorption of Hg(II) ions than the other metal ions. Also, the SnO_2-ZnO-eggshell nanocomposites could be recycled three times without considerable loss in their adsorption activity. The high stability and durability of SnO_2-ZnO-eggshell nanocomposites during the adsorption process were confirmed by the comparison of the TEM image of the reused nanocomposites after three cycles with fresh ones. Generally, SnO_2-ZnO-eggshell nanocomposites were the efficient and green-based adsorbent for the removal of Hg(II) ions. The present study includes diverse advantages such as eco-friendly protocol, optimal use of biowaste materials, simple conditions and excellent adsorption capacities as same as short adsorption times.

Acknowledgements The authors gratefully acknowledge the Birjand University of Technology and the research deputy of Zahedan University of Medical Sciences for approval and financial support of the current study. This project was approved in the Ethics Committee of Zahedan University of Medical Sciences, code IR.ZAUMS.REC.1398.385.

Compliance with ethical standards

Conflict of interest All authors declare that they have no conflict of interest.

References

1. Ullrich SM, Tanton TW, Abdrashitova SA. Mercury in the aquatic environment: a review of factors affecting methylation. Crit Rev Environ Sci Technol. 2001;31:241–93. https://doi.org/10.1080/20016491089226.
2. Tibau AV, Grube BD. Mercury contamination from dental amalgam. J Heal Pollut. 2019;9:190612–33. https://doi.org/10.5696/2156-9614-9.22.190612.
3. Sobhanardakani S, Jafari A, Zandipak R, Meidanchi A. Removal of heavy metal (Hg(II) and Cr(VI)) ions from aqueous solutions using Fe_2O_3@SiO_2 thin films as a novel adsorbent. Process Saf Environ Prot. 2018;120:348–57. https://doi.org/10.1016/j.psep.2018.10.002.
4. Uçar Y, Brantley WA. Biocompatibility of dental amalgams. Int J Dent. 2011;2011:981595–602. https://doi.org/10.1155/2011/981595.
5. Sharma A, Sharma A, Arya RK. Removal of Mercury(II) from Aqueous Solution: a Review of Recent Work. Sep Sci Technol. 2015;50:1310–20. https://doi.org/10.1080/01496395.2014.968261.
6. Von Canstein H, Li Y, Timmis KN, Deckwer WD, Wagner-Döbler I. Removal of mercury from chloralkali electrolysis wastewater by a mercury-resistant Pseudomonas putida strain. Appl Environ Microbiol. 1999;65:5279–84. https://doi.org/10.1128/aem.65.12.5279-5284.1999.
7. Wang J, Hong Y, Lin Z, Zhu C, Da J, Chen G, et al. A novel biological sulfur reduction process for mercury-contaminated wastewater treatment. Water Res. 2019;160:288–95. https://doi.org/10.1016/j.watres.2019.05.066.
8. Bidhendi ME, Nabi Bidhendi GR, Mehrdadi N, Rashedi H. Modified Mesoporous Silica (SBA-15) with Trithiane as a new effective adsorbent for mercury ions removal from aqueous environment. J Environ Heal Sci Eng. 2014;12:1–6. https://doi.org/10.1186/2052-336X-12-100.
9. Lone S, Yoon DH, Lee H, Cheong IW. Gelatin-chitosan hydrogel particles for efficient removal of Hg(ii) from wastewater. Environ Sci Water Res Technol. 2019;5:83–90. https://doi.org/10.1039/c8ew00678d.
10. Bhosale TT, Shinde HM, Gavade NL, Babar SB, Gawade VV, Sabale SR, et al. Biosynthesis of SnO_2 nanoparticles by aqueous leaf extract of Calotropis gigantea for photocatalytic applications. J Mater Sci Mater Electron. 2018;29:6826–34. https://doi.org/10.1007/s10854-018-8669-0.
11. Chen T, Quan X, Ji Z, Li X, Pei Y. Science of the total environment synthesis and characterization of a novel magnetic calcium-rich nanocomposite and its remediation behaviour for As (III) and Pb (II) co-contamination in aqueous systems 2020;706:135122–33. https://doi.org/10.1016/j.scitotenv.2019.135122.
12. Ahmadi E, Shokri B, Mesdaghinia A, Nabizadeh R, Reza Khani M, Yousefzadeh S, et al. Synergistic effects of α-Fe_2O_3-TiO_2 and $Na_2S_2O_8$ on the performance of a non-thermal plasma reactor as a novel catalytic oxidation process for dimethyl phthalate degradation. Sep Purif Technol. 2020;250:117185. https://doi.org/10.1016/j.seppur.2020.117185.
13. Aghajari N, Ghasemi Z, Younesi H, Bahramifar N. Synthesis, characterization and photocatalytic application of Ag-doped Fe-ZSM-5@TiO_2 nanocomposite for degradation of reactive red 195 (RR 195) in aqueous environment under sunlight irradiation. J Environ Health Sci Eng. 2019;17:219–32. https://doi.org/10.1007/s40201-019-00342-5.
14. Honarmand M, Golmohammadi M, Naeimi A. Biosynthesis of tin oxide (SnO_2) nanoparticles using jujube fruit for photocatalytic degradation of organic dyes. Adv Powder Technol. 2019;30:1551–7. https://doi.org/10.1016/j.apt.2019.04.033.
15. Balcha A, Yadav OP, Dey T. Photocatalytic degradation of methylene blue dye by zinc oxide nanoparticles obtained from precipitation and sol-gel methods. Environ Sci Pollut Res. 2016;23:25485–93. https://doi.org/10.1007/s11356-016-7750-6.
16. Chauhan AK, Kataria N, Garg VK. Green fabrication of ZnO nanoparticles using Eucalyptus spp. leaves extract and their application in wastewater remediation. Chemosphere. 2020;247:125803. https://doi.org/10.1016/j.chemosphere.2019.125803.
17. Hu JQ, Li Q, Meng XM, Lee CS, Lee ST. Thermal reduction route to the fabrication of coaxial Zn/ZnO nanocables and ZnO nanotubes. Chem Mater. 2003;15:305–8. https://doi.org/10.1021/cm020649y.
18. Wang Z, Song D, Si J, Jiang Y, Yang Y, Jiang Y, et al. One-step hydrothermal reduction synthesis of tiny Sn/SnO2 nanoparticles sandwiching between spherical graphene with excellent lithium storage cycling performances. Electrochim Acta. 2018;292:72–80. https://doi.org/10.1016/j.electacta.2018.09.141.
19. Reuge N, Bacsa R, Serp P, Caussat B. Chemical vapor synthesis of zinc oxide nanoparticles: experimental and preliminary modeling studies. J Phys Chem C. 2009;113:19845–52. https://doi.org/10.1021/jp9070955.
20. Nagirnyak SV, Lutz VA, Dontsova TA, Astrelin IM. Synthesis and Characterization of Tin(IV) Oxide Obtained by Chemical Vapor Deposition Method. Nanoscale Res Lett. 2016;11:343–9. https://doi.org/10.1186/s11671-016-1547-x.
21. Aziz M, Saber Abbas S, Wan Baharom WR. Size-controlled synthesis of SnO_2 nanoparticles by sol-gel method. Mater Lett. 2013;91:31–4. https://doi.org/10.1016/j.matlet.2012.09.079.

22. Hasnidawani JN, Azlina HN, Norita H, Bonnia NN, Ratim S, Ali ES. Synthesis of ZnO Nanostructures Using Sol-Gel Method. Procedia Chem. 2016;19:211–6. https://doi.org/10.1016/j.proche.2016.03.095.
23. Barreto GP, Morales G, Quintanilla MLL. Microwave Assisted Synthesis of ZnO Nanoparticles: Effect of Precursor Reagents, Temperature, Irradiation Time, and Additives on Nano-ZnO Morphology Development. J Mater. 2013;2013:1–11. https://doi.org/10.1155/2013/478681.
24. Nehru LC, Sanjeeviraja C. Rapid synthesis of nanocrystalline SnO_2 by a microwave-assisted combustion method. J Adv Ceram. 2014;3:171–6. https://doi.org/10.1007/s40145-014-0101-5.
25. Zamand N, Nakhaei Pour A, Housaindokht MR, Izadyar M. Size-controlled synthesis of SnO_2 nanoparticles using reverse microemulsion method. Solid State Sci. 2014;33:6–11. https://doi.org/10.1016/j.solidstatesciences.2014.04.005.
26. Yildirim ÖA, Durucan C. Synthesis of zinc oxide nanoparticles elaborated by microemulsion method. J Alloys Compd. 2010;506:944–9. https://doi.org/10.1016/j.jallcom.2010.07.125.
27. Al-Dahash G, Mubdir Khilkala W, Abdul Vahid SN. Preparation and characterization of ZnO nanoparticles by laser ablation in NaOH aqueous solution. Iran J Chem Chem Eng. 2018;37:11–6.
28. Hadi AJ. Study of the Effect of laser Pulses on Synthesis of SnO_2 Nanoparticles by Laser Ablation in Methanol. Eng Technol J. 2014;32:1059–67.
29. Yang H, Hu Y, Tang A, Jin S, Qiu G. Synthesis of tin oxide nanoparticles by mechanochemical reaction. J Alloys Compd. 2004;363:271–4. https://doi.org/10.1016/S0925-8388(03)00473-0.
30. Damonte LC, Mendoza Zélis LA, Marí Soucase B, Hernández Fenollosa MA. Nanoparticles of ZnO obtained by mechanical milling. Powder Technol. 2004;148:15–9. https://doi.org/10.1016/j.powtec.2004.09.014.
31. Ebrahimian J, Mohsennia M, Khayatkashani M. Photocatalytic-degradation of organic dye and removal of heavy metal ions using synthesized SnO_2 nanoparticles by Vitex agnus-castus fruit via a green route. Mater Lett. 2020;263:127255. https://doi.org/10.1016/j.matlet.2019.127255.
32. Ehrampoush MH, Miria M, Salmani MH, Mahvi AH. Cadmium removal from aqueous solution by green synthesis iron oxide nanoparticles with tangerine peel extract. J Environ Heal Sci Eng. 2015;13:1–7. https://doi.org/10.1186/s40201-015-0237-4.
33. Bahramikia S, Yazdanparast R. Phytochemistry and medicinal properties of teucrium polium L. (Lamiaceae). Phyther Res. 2012;26:1581–93. https://doi.org/10.1002/ptr.4617.
34. Hashemi SF, Tasharrofi N, Saber MM. Green synthesis of silver nanoparticles using Teucrium polium leaf extract and assessment of their antitumor effects against MNK45 human gastric cancer cell line. J Mol Struct. 2020;1208:127889. https://doi.org/10.1016/j.molstruc.2020.127889.
35. Kravchenko GV, Domoroshchina EN, Kuz'micheva GM, Gaynanova AA, Amarantov SV, Pirutko LV, et al. Zeolite–titanium dioxide nanocomposites: preparation, characterization, and adsorption properties. Nanotechnologies Russ. 2016;11:579–92. https://doi.org/10.1134/S1995078016050098.
36. Honarmand M, Golmohammadi M, Naeimi A. Green synthesis of SnO_2-bentonite nanocomposites for the efficient photodegradation of methylene blue and eriochrome black-T. Mater Chem Phys. 2020;241:122416–26. https://doi.org/10.1016/j.matchemphys.2019.122416.
37. Abdul-Raheim ARM, El-Saeed Shimaa M, Farag RK, Abdel-Raouf Manar E. Low cost biosorbents based on modified starch iron oxide nanocomposites for selective removal of some heavy metals from aqueous solutions. Adv Mater Lett. 2016;7:402–9. https://doi.org/10.5185/amlett.2016.6061.
38. Bharathi D, Ranjithkumar R, Vasantharaj S, Chandarshekar B, Bhuvaneshwari V. Synthesis and characterization of chitosan/iron oxide nanocomposite for biomedical applications. Int J Biol Macromol. 2019;132:880–7. https://doi.org/10.1016/j.ijbiomac.2019.03.233.
39. Khalid A, Khan R, Ul-Islam M, Khan T, Wahid F. Bacterial cellulose-zinc oxide nanocomposites as a novel dressing system for burn wounds. Carbohydr Polym. 2017;164:214–21. https://doi.org/10.1016/j.carbpol.2017.01.061.
40. Sun Z, Yao G, Liu M, Zheng S. In situ synthesis of magnetic $MnFe_2O_4$/diatomite nanocomposite adsorbent and its efficient removal of cationic dyes. J Taiwan Inst Chem Eng. 2017;71:501–9. https://doi.org/10.1016/j.jtice.2016.12.013.
41. He Q, Zhang Y, Cai X, Wang S. Fabrication of gelatin-TiO_2 nanocomposite film and its structural, antibacterial and physical properties. Int J Biol Macromol. 2016;84:153–60. https://doi.org/10.1016/j.ijbiomac.2015.12.012.
42. Ramanathan S, Selvin SP, Obadiah A, Durairaj A, Santhoshkumar P, Lydia S, et al. Synthesis of reduced graphene oxide/ZnO nanocomposites using grape fruit extract and Eichhornia crassipes leaf extract and a comparative study of their photocatalytic property in degrading Rhodamine B dye. J Environ Heal Sci Eng. 2019;17:195–207. https://doi.org/10.1007/s40201-019-00340-7.
43. Ahmaruzzaman M, Gupta VK. Rice husk and its ash as low-cost adsorbents in water and wastewater treatment. Ind Eng Chem Res. 2011;50:13589–613. https://doi.org/10.1021/ie201477c.
44. Carvalho J, Araujo J, Castro F. Alternative low-cost adsorbent for water and wastewater decontamination derived from eggshell waste: an overview. Waste Biomass Valoriz. 2011;2:157–67. https://doi.org/10.1007/s12649-010-9058-y.
45. Matouq M, Jildeh N, Qtaishat M, Hindiyeh M, Al Syouf MQ. The adsorption kinetics and modeling for heavy metals removal from wastewater by Moringa pods. J Environ Chem Eng. 2015;3:775–84. https://doi.org/10.1016/j.jece.2015.03.027.
46. Mondal DK, Nandi BK, Purkait MK. Removal of mercury (II) from aqueous solution using bamboo leaf powder: equilibrium, thermodynamic and kinetic studies. J Environ Chem Eng. 2013;1:891–8. https://doi.org/10.1016/j.jece.2013.07.034.
47. Coelho GF, Gonçalves AC, Tarley CRT, Casarin J, Nacke H, Franczis kowski MA. Removal of metal ions Cd (II), Pb (II), and Cr (III) from water by the cashew nut shell Anacardium occidentale L. Ecol Eng. 2014;73:514–25. https://doi.org/10.1016/j.ecoleng.2014.09.103.
48. Hossain MA, Ngo HH, Guo WS, Nguyen TV. Palm oil fruit shells as biosorbent for copper removal from water and wastewater: experiments and sorption models. Bioresour Technol. 2012;113:97–101. https://doi.org/10.1016/j.biortech.2011.11.111.
49. Nasrollahzadeh M, Sajadi SM, Hatamifard A. Waste chicken eggshell as a natural valuable resource and environmentally benign support for biosynthesis of catalytically active Cu/eggshell, Fe_3O_4/eggshell and Cu/Fe_3O_4/eggshell nanocomposites. Appl Catal B Environ. 2016;191:209–27. https://doi.org/10.1016/j.apcatb.2016.02.042.
50. Golmohammadi M, Honarmand M, Ghanbari S. A green approach to synthesis of ZnO nanoparticles using jujube fruit extract and their application in photocatalytic degradation of organic dyes. Spectrochim Acta - Part A Mol Biomol Spectrosc. 2020;229:117961–9. https://doi.org/10.1016/j.saa.2019.117961.
51. Shahraki BK, Mehrabi B, Gholizadeh K, Mohammadinasab M. Thermal behavior of calcite as an expansive agent. J Min Metall Sect B Metall. 2011;47:89–97. https://doi.org/10.2298/JMMB1101089S.
52. Wang Q, Li J, Zhang C, Qu X, Liu J, Yang Z. Regenerative superhydrophobic coating from microcapsules. J Mater Chem. 2010;20:3211–5. https://doi.org/10.1039/b925298c.
53. Yuvakkumar R, Hong SI. Incubation and aging effect on cassiterite type tetragonal rutile SnO_2 nanocrystals. J Mater Sci Mater

Electron. 2015;26:2305–10. https://doi.org/10.1007/s10854-015-2684-1.
54. Jayaprada P, Rao MC, Pardhasaradhi P, Datta Prasad PV, Manepalli RKNR, Pisipati VGKM. Optical studies of n-octyloxy-cyanobiphenyl (8ocb) with dispersed ZnO nanoparticles for display device application. Optik (Stuttg). 2019;185:1226–37. https://doi.org/10.1016/j.ijleo.2019.04.060.
55. Okpala CC. Nanocomposites – An Overview. Int J Eng Res Dev. 2013;8:17–23.
56. Ahmadi E, Kakavandi B, Azari A, Izanloo H, Gharibi H, Mahvi AH, et al. The performance of mesoporous magnetite zeolite nanocomposite in removing dimethyl phthalate from aquatic environments. Desalin Water Treat. 2016;57:27768–82. https://doi.org/10.1080/19443994.2016.1178174.
57. Fu L, Wang S, Lin G, Zhang L, Liu Q, Fang J, et al. Post-functionalization of UiO-66-NH_2 by 2,5-Dimercapto-1,3,4-thiadiazole for the high efficient removal of Hg(II) in water. J Hazard Mater. 2019;368:42–51. https://doi.org/10.1016/j.jhazmat.2019.01.025.
58. Mobasherpour I, Salahi E, Pazouki M. Removal of divalent cadmium cations by means of synthetic nano crystallite hydroxyapatite. Desalination. 2011;266:142–8. https://doi.org/10.1016/j.desal.2010.08.016.
59. Lin G, Wang S, Zhang L, Hu T, Peng J, Cheng S, et al. Selective and high efficient removal of Hg^{2+} onto the functionalized corn bract by hypophosphorous acid. J Clean Prod. 2018;192:639–46. https://doi.org/10.1016/j.jclepro.2018.05.043.
60. Mahdavi S, Jalali M, Afkhami A. Removal of heavy metals from aqueous solutions using Fe_3O_4, ZnO, and CuO nanoparticles. J Nanoparticle Res. 2012;14:846–64. https://doi.org/10.1007/s11051-012-0846-0.
61. Naushad M, Vasudevan S, Sharma G, Kumar A, Alothman ZA. Adsorption kinetics, isotherms, and thermodynamic studies for Hg^{2+} adsorption from aqueous medium using alizarin red-S-loaded amberlite IRA-400 resin. Desalin Water Treat. 2016;57:18551–9. https://doi.org/10.1080/19443994.2015.1090914.
62. Moghaddam HK, Pakizeh M. Experimental study on mercury ions removal from aqueous solution by MnO_2/CNTs nanocomposite adsorbent. J Ind Eng Chem. 2015;21:221–9. https://doi.org/10.1016/j.jiec.2014.02.028.
63. Diagboya PN, Olu-Owolabi BI, Adebowale KO. Synthesis of covalently bonded graphene oxide-iron magnetic nanoparticles and the kinetics of mercury removal. RSC Adv. 2015;5:2536–42. https://doi.org/10.1039/c4ra13126f.
64. Sreeprasad TS, Maliyekkal SM, Lisha KP, Pradeep T. Reduced graphene oxide-metal/metal oxide composites: facile synthesis and application in water purification. J Hazard Mater. 2011;186:921–31. https://doi.org/10.1016/j.jhazmat.2010.11.100.
65. Fu W, Huang Z. One-pot Synthesis of Two-dimensional Porous Fe_3O_4/poly($C_3N_3S_3$) Network Nanocomposite for Selective Removal of Pb(II) and Hg(II) from Synthetic Wastewater One-pot Synthesis of Two-dimensional Porous Fe_3O_4/poly($C_3N_3S_3$). Network Nanoco. 2018;6:14785–94. https://doi.org/10.1021/acssuschemeng.8b03320.
66. Li R, Liu L, Yang F. Removal of aqueous Hg(II) and Cr(VI) using phytic acid doped polyaniline/cellulose acetate composite membrane. J Hazard Mater. 2014;280:20–30. https://doi.org/10.1016/j.jhazmat.2014.07.052.
67. Guo X, Du B, Wei Q, Yang J, Hu L, Yan L, et al. Synthesis of amino functionalized magnetic graphenes composite material and its application to remove Cr(VI), Pb(II), Hg(II), Cd(II) and Ni(II) from contaminated water. J Hazard Mater. 2014;278:211–20. https://doi.org/10.1016/j.jhazmat.2014.05.075.
68. Anirudhan TS, Shainy F. Effective removal of mercury(II) ions from chlor-alkali industrial wastewater using 2-mercaptobenzamide modified itaconic acid-grafted-magnetite nanocellulose composite. J Colloid Interface Sci. 2015;456:22–31. https://doi.org/10.1016/j.jcis.2015.05.052.
69. Abdelrahman EA, Subaihi A. Application of Geopolymers Modified with Chitosan as Novel Composites for Efficient Removal of Hg(II), Cd(II), and Pb(II) Ions from Aqueous Media. J Inorg Organomet Polym Mater. 2020;30:2440–63. https://doi.org/10.1007/s10904-019-01380-0.
70. Saleh TA, Sari A, Tuzen M. Optimization of parameters with experimental design for the adsorption of mercury using polyethylenimine modified-activated carbon. J Environ Chem Eng. 2017;5:1079–88. https://doi.org/10.1016/j.jece.2017.01.032.